

Britta Basse · Bruce C. Baguley · Elaine S. Marshall · Wayne R. Joseph
Bruce van Brunt · Graeme Wake · David J.N. Wall

Modelling cell death in human tumour cell lines exposed to the anticancer drug paclitaxel

Received: 24 June 2003 / Revised version: 9 October 2003 /
Published online: 6 February 2004 – © Springer-Verlag 2004

Abstract. Most anti-cancer drugs in use today exert their effects by inducing a programmed cell death mechanism. This process, termed apoptosis, is accompanied by degradation of the DNA and produces cells with a range of DNA contents. We have previously developed a phase transition mathematical model to describe the mammalian cell division cycle in terms of cell cycle phases and the transition rates between these phases. We now extend this model here to incorporate a transition to a programmed cell death phase whereby cellular DNA is progressively degraded with time. We have utilised the technique of flow cytometry to analyse the behaviour of a melanoma cell line (NZM13) that was exposed to paclitaxel, a drug used frequently in the treatment of cancer. The flow cytometry profiles included a complex mixture of living cells whose DNA content was increasing with time and dying cells whose DNA content was decreasing with time. Application of the mathematical model enabled estimation of the rate constant for entry of mitotic cells into apoptosis (0.035 per hour) and the duration of the period of DNA degradation (51 hours). These results provide a dynamic model of the action of an anticancer drug that can be extended to improve the clinical outcome in individual cancer patients.

1. Introduction

The cancer cell division cycle can be divided into four distinct phases, namely G_1 -phase, DNA synthesis or S -phase, G_2 -phase and mitosis or M -phase (Fig. 1). The transitions between these phases are largely controlled by stochastic processes and we have developed a mathematical model to describe these phases and the transitions rates between them ([2]). Anticancer drugs used in the treatment of cancer generally affect cancer cells by inducing a combination of programmed cell death, termed apoptosis, and cell cycle arrest. Paclitaxel, an anticancer drug commonly

B. Baguley, E. Marshall, W. Joseph: Auckland Cancer Society Research Centre, Faculty of Medical and Health Sciences, University of Auckland, Private Bag 92019, Auckland, New Zealand.

B. Basse, G. Wake, D. Wall: Biomathematics Research Centre, University of Canterbury, Private Bag 4800, Christchurch, New Zealand.
e-mail: b.basse@math.canterbury.ac.nz

B. van Brunt: Institute of Fundamental Sciences, Massey University, Private Bag 11 222, Palmerston North, New Zealand.

Key words or phrases: Human tumour cells – Cell division cycle – Mathematical model – Cell death – Apoptosis – Flow cytometry – Steady size distribution – Fredholm integral equation – Mitotic arrest – Paclitaxel

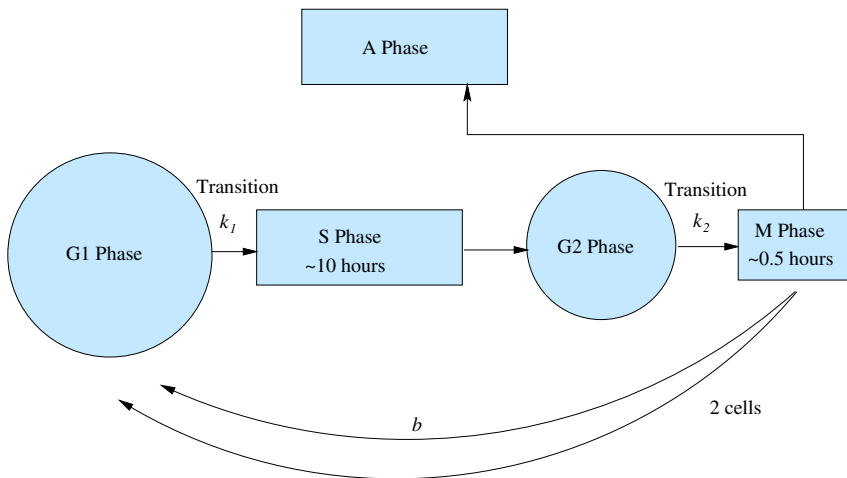


Fig. 1. Cell cycle control.

used to treat ovarian and other types of cancer, arrests cancer cells at the stage of mitosis, where the chromosomes of the daughter cells are segregated prior to cell division. Apoptosis occurs subsequent to mitotic arrest ([7]) and is thought to account for the therapeutic properties of paclitaxel. The clinical response to paclitaxel varies considerably in different patients and in different types of cancer, suggesting that the degree of induction of apoptosis in individual cancers can vary. In the melanoma line that we used previously for the development of the mathematical model ([2]), we found little evidence of apoptosis and this process was omitted from the model. In this report, we have studied a cancer cell line that shows evidence of both cell cycle arrest and apoptosis in response to paclitaxel.

The induction of apoptosis in cultured cells is accompanied by the appearance of cells with partially degraded DNA, which can be observed by flow cytometry ([18]). In order to describe this induction of apoptosis, we define here a model where *M*-phase cells undergo a stochastic transition to a phase we term *A*-phase, in which DNA is degraded with time. This model enables us to calculate, the rate of entry of mitotic cells into *A*-phase, the rate of DNA degradation with time during *A*-phase and the rate of eventual cell loss. The model generates a series of flow cytometry profiles that can be compared with experimental data. It also provides new insights on how paclitaxel acts on tumour cells and has the potential to further our understanding of this drug.

For clarity, we give an overview of the paper: Firstly, in section 2.1 we introduce a generalised size structured model for a cell population. In section 2.2 we consider the model for a cell line unperturbed by cancer therapy. We look for separable solutions of this model and we find these in a ‘no dispersion’ case in section 2.2.1. For the dispersion case, section 2.2.2, the problem is reduced to solving a Fredholm integral equation. We discuss the numerics of this in section 2.2.3. We summarise the uniqueness and attractiveness of our model solutions in section 2.2.4. In section

2.3 we model the addition of the anticancer drug paclitaxel to an unperturbed cell population. We then compare model outputs to those obtained experimentally in sections 3 and 4. Finally, in section 5 we discuss the biological significance of our results.

We aim to describe the effects of exposure of an unperturbed cancer cell line growing in culture to paclitaxel, an anticancer drug. The mode of analysis is as follows: A cohort of cells has its DNA content measured using the technique of flow cytometry. This involves staining of the cellular DNA with a fluorescent dye and then measuring the fluorescence of each cell in a flow cytometer. Since fluorescence is proportional to DNA content, a frequency histogram (or DNA distribution profile) can be obtained where cells are binned according to their DNA content at various ‘snapshots’ in time. When cells are in a logarithmic or exponential growth phase, the shape of the DNA profile does not change. Starting from this steady DNA distribution (SDD), the cell line is perturbed by the addition of an anticancer drug. Further flow cytometry DNA profiles at discrete later times provide a series of ‘snapshots’ of the effects of the treatment. Drug-induced perturbation of some cell lines may cause arrest of cells at certain phases of the cell cycle, leading to an accumulation of cells with this DNA content. It may also cause a proportion to undergo apoptosis, whereupon their DNA content is reduced with time.

2. Mathematical model

2.1. Generalised model equations

In [2] we devised a mathematical model for the cell division cycle in which the rate of transition to cell death was set at zero. We now extend this model to incorporate a transition from mitosis to cell death. This extension will enable us to model the addition of paclitaxel, an anticancer drug that induces not only mitotic arrest but also subsequent cell death.

For the mathematical model we choose five compartments representing the sub-populations of cells, G_1 , S , G_2 , M , and A distinguished by their position within the cell cycle compartments for G_1 -phase, S -phase, G_2 -phase, M -phase and A -phase respectively (Fig. 1). Our model equations, with appropriate initial and boundary conditions, are:

G_1 -phase:

$$\frac{\partial G_1}{\partial t}(x, t) = 4bM(2x, t) - k_1G_1(x, t), \quad t > 0, \quad 0 < x < L, \quad (1)$$

$$G_1(x, 0) = G_{10}(x), \quad 0 < x < L. \quad (2)$$

S -phase:

$$S(x, t) = \int_0^{T_S} \bar{S}(x, t; \tau_S) d\tau_S, \quad (3)$$

where $\bar{S}(x, t; \tau_S)$ represents cells that have been in S phase for τ_S hours and is the solution of the partial differential equation:

$$\begin{aligned} \frac{\partial \bar{S}}{\partial t}(x, t; \tau_S) + \frac{\partial \bar{S}}{\partial \tau_S}(x, t; \tau_S) \\ = D \frac{\partial^2 \bar{S}}{\partial x^2}(x, t; \tau_S) - g \frac{\partial \bar{S}}{\partial x}(x, t; \tau_S), \quad t, \tau_S > 0, \quad 0 < x < L, \end{aligned} \quad (4)$$

with side conditions:

$$\bar{S}(x, t; \tau_S = 0) = k_1 G_1(x, t), \quad t > 0, \quad 0 < x < L, \quad (5)$$

$$\bar{S}(x, t = 0; \tau_S) = \bar{S}_{0\tau_S}(x, \tau_S), \quad \tau_S > 0, \quad 0 < x < L, \quad (6)$$

$$D \frac{\partial \bar{S}}{\partial x}(0, t; \tau_S) - g \bar{S}(0, t; \tau_S) = 0, \quad t, \tau_S > 0, \quad (7)$$

$$D \frac{\partial \bar{S}}{\partial x}(L, t; \tau_S) - g \bar{S}(L, t; \tau_S) = 0, \quad t, \tau_S > 0. \quad (8)$$

Thus the initial distribution for cells in S -phase is:

$$\begin{aligned} S(x, t = 0) = S_0(x) &= \int_0^{T_S} \bar{S}(x, t = 0; \tau_S) d\tau_S \\ &= \int_0^{T_S} \bar{S}_{0\tau_S}(x, \tau_S) d\tau_S, \quad \tau_S > 0, \quad 0 < x < L. \end{aligned} \quad (9)$$

G₂-phase:

$$\frac{\partial G_2}{\partial t}(x, t) = \bar{S}(x, t; T_S) - k_2 G_2(x, t), \quad t > 0, \quad 0 < x < L, \quad (10)$$

$$G_2(x, 0) = G_{20}(x), \quad 0 < x < L. \quad (11)$$

M-phase:

$$M(x, t) = \int_0^\infty \bar{M}(x, t; \tau_M) d\tau_M, \quad (12)$$

where $\bar{M}(x, t; \tau_M)$ represents cells that have been in M phase for τ_M hours and is the solution of

$$\begin{aligned} \frac{\partial \bar{M}}{\partial t}(x, t; \tau_M) + \frac{\partial \bar{M}}{\partial \tau_M}(x, t; \tau_M) \\ = -b \bar{M}(x, t; \tau_M) - \mu_M \bar{M}(x, t; \tau_M), \quad t, \tau_M > 0, \quad 0 < x < L, \end{aligned} \quad (13)$$

with side conditions

$$\bar{M}(x, t; \tau_M = 0) = k_2 G_2(x, t), \quad t > 0, \quad 0 < x < L, \quad (14)$$

$$\bar{M}(x, t = 0; \tau_M) = \bar{M}_{0\tau_M}(x, \tau_M), \quad \tau_M > 0, \quad 0 < x < L. \quad (15)$$

Thus the initial distribution for cells in M -phase is:

$$\begin{aligned} M(x, t = 0) &= M_0(x) = \int_0^\infty \bar{M}(x, t = 0; \tau_M) d\tau_M \\ &= \int_0^\infty \bar{M}_{0\tau_M}(x, \tau_M) d\tau_M, \quad \tau_M > 0, \quad 0 < x < L. \end{aligned} \quad (16)$$

A-phase:

$$\frac{\partial A}{\partial t}(x, t) = g_A \frac{\partial A}{\partial x}(x, t) + \int_{T_M}^t \mu_M \bar{M}(x, t; \tau_M) d\tau_M, \quad t, \tau_M > 0, \quad 0 < x < L, \quad (17)$$

$$A(x, 0) = A_0, \quad 0 < x < L, \quad (18)$$

$$A(L, t) = 0, \quad t > 0. \quad (19)$$

For a detailed description of the model, excluding apoptosis, we refer the reader to [2]. For completeness, we give a brief description here and a summary of parameters and their descriptions in Table 1. The model equations are generic and provide

Table 1. Model parameters and variables. Mesh size: $\Delta t=0.5$; $\Delta x = .01$; $x_{max}=2.5$. LB and UB are the lower and upper bounds respectively as applied during the optimisation routine of fitting model outputs to those obtained experimentally.

Parameter (Dim.)	Description	Value	LB	UB
x ([L])	relative DNA content			
t (hours)	time			
$G_1(x, t)$	number density of cells in G_1 -phase			
$S(x, t)$	number density of cells in S -phase			
$G_2(x, t)$	number density of cells in G_2 -phase			
$M(x, t)$	number density of cells in M -phase			
$A(x, t)$	number density of cells in A -phase			
k_1 ($\frac{1}{[t]}$)	transition probability of cells from G_1 to S -phase		4×10^{-4}	1
D ($\frac{[x]^2}{[t]}$)	dispersion coefficient	4×10^{-4}		
$g = \frac{1}{T_S}$ ($\frac{[x]}{[t]}$)	average growth rate of DNA in S -phase	0.1		
$T_S = \frac{1}{g}$ (hours)	time in S -phase	10		
k_2 ($\frac{1}{[t]}$)	transition probability of cells from G_2 to M -phase		4×10^{-4}	1
b ($\frac{1}{[t]}$)	division rate	2		
μ_M ($\frac{1}{[t]}$)	eventual death rate in M -phase		0	1
g_A ($\frac{[x]}{[t]}$)	average disintegration rate of DNA in A -phase		0	$2/\Delta t$
T_M (hours)	time in M -phase before apoptosis onset		0	40
T_c (hours)	total cell cycle time		12	250

the basis for modelling cell lines both unperturbed and perturbed by a range of cancer treatments. The time variables, t , τ_S and τ_M , are measured in hours while x , relative DNA content, is dimensionless and is assumed to be smaller than some maximum DNA content $L \in \mathbb{R}^+$. All parameters in the model may be functions of (one or more of) t , τ_S , τ_M and x but for the scope of this paper it is sufficient to consider only constant parameter values. Initial distributions in each phase, $G_1(x, t = 0)$, $\bar{S}(x, t = 0, \tau_S)$, $G_2(x, t = 0)$, $\bar{M}(x, t = 0, \tau_M)$ and $A(x, t = 0)$ at time $t = 0$, are the arbitrary (positive) functions: $G_{10}(x)$, $\bar{S}_{0\tau_S}(x, \tau_S)$, $G_{20}(x)$, $\bar{M}_{0\tau_M}(x, \tau_M)$ and $A_0(x)$ respectively. Boundary conditions in \bar{S} -phase and A -phase, expressions (7), (8) and (19) respectively, ensure that cells do not travel into the infeasible region ($x < 0$ or $x > L$) during times in these phases. The integrals of equations (3), (9), (12) and (16) represent summation over previous time and do not violate causality.

From G_1 -phase, equation (1), cells transit to S -phase with transition probability k_1 . Newly divided cells from M -phase join G_1 -phase at a rate of b divisions per unit time.

During S -phase, equations (3)–(9), the parameter g is the average rate of increase of DNA content during S -phase. The dispersion parameter, D , has two roles, firstly, it accounts for the apparent variation in DNA content caused by flow cytometry and the fact that cells are not always illuminated evenly when they pass through a laser beam in a flow cytometer. Secondly, many human tumours exhibit genetic instability that can result in changes to the chromosomal complement (and thus of DNA content) of individual cells ([8]).

The length of time that human tumour cells spend in S -phase, T_S , varies in different cell lines but is typically 10 hours in a melanoma line ([2]). The time in S -phase, T_S , is related to the parameter g , the average rate of increase of DNA during S -phase, by the equation $T_S = 1/g$ hours ([17]). This gives us the integral relation of equation (3) for cells in S phase. It can be shown (see [2]) that:

1. The case $D = 0$,

$$\bar{S}(x, t; \tau_S) = \begin{cases} k_1 G_1(x - g\tau_S, t - \tau_S), & t - \tau_S \geq 0, \quad x > g\tau_S, \\ 0, & t - \tau_S < 0 \quad \text{or} \quad x \leq g\tau_S. \end{cases} \quad (20)$$

2. The case $D \neq 0$,

$$\bar{S}(x, t; \tau_S) = \begin{cases} \int_0^L k_1 G_1(z, t - \tau_S) \gamma(\tau_S, x, z) dz, & t - \tau_S \geq 0, \\ 0, & t - \tau_S < 0, \end{cases} \quad (21)$$

where $L \in \mathbb{R}^+$, is some large positive number, representing maximum DNA content, and

$$\gamma(\tau_S, x, z) \approx \frac{1}{\sqrt{4\pi D\tau_S}} \left(e^{-((x-g\tau_S)-z)^2/4D\tau_S} \right), \quad (22)$$

(see appendix, equation (103)). Thus, the number density of cells in S -phase, $S(x, t)$ can be found in terms of G_1 -phase cells in both cases as:

1. Case $D = 0$,

$$S(x, t) \approx \begin{cases} \int_0^{t_1} k_1 G_1(x - g\tau_S, t - \tau_S) d\tau_S, & t - \tau_S \geq 0, \quad x > g\tau_S, \\ 0, & x \leq g\tau_S. \end{cases} \quad (23)$$

2. Case $D \neq 0$,

$$S(x, t) \approx \begin{cases} k_1 G_1(x, t) + \int_0^{t_1} \int_0^L k_1 G_1(z, t - \tau_S) \\ \quad \times \gamma(\tau_S, x, z) dz d\tau_S, & t - \tau_S \geq 0, \\ 0, & t - \tau_S < 0, \end{cases} \quad (24)$$

where

$$t_1 = \begin{cases} T_S, & t \geq T_S, \\ t, & t < T_S. \end{cases} \quad (25)$$

It should be noted that we can combine equations (3) and (4) to give one partial differential equation for cells in S -phase

$$\frac{\partial S}{\partial t}(x, t) = D \frac{\partial^2 S}{\partial x^2} - g \frac{\partial S}{\partial x}(x, t) + k_1 G_1(x, t) - \bar{S}(x, t; T_S), \quad (26)$$

with zero flux boundary conditions corresponding to equations (7) and (8),

$$D \frac{\partial S}{\partial x}(0, t) - gS(0, t) = 0, \quad t > 0, \quad (27)$$

$$D \frac{\partial S}{\partial x}(L, t) - gS(L, t) = 0, \quad t > 0, \quad (28)$$

respectively.

The source term, $\bar{S}(x, t; \tau_S = T_S)$, in equation (10) represents cells that have been in S -phase for T_S hours. The transition rate of cells from G_2 -phase to M -phase is k_2 . Cells that have been in M -phase for τ_M hours enter A -phase with transition probability μ_M . This gives rise to the loss term in equation (13). We assume that $\mu_M = 0$ when $\tau_M < T_M$. Generally, μ_M will increase as τ_M increases but as a first approximation we assume μ_M is constant after time T_M .

Finally, equation (17) depicts the removal phase for A -phase cells and is similar to equation (4) (S -phase) in that the DNA content of a cell changes in time. In equation (4) the DNA content increases corresponding to DNA synthesis whereas during A -phase the DNA content of a cell decreases, representing DNA degradation. The average rate of DNA degradation during A -phase is g_A per unit time and there is no dispersion. Since cells disappear as x approaches 0, for simulations we impose the condition $A(0, t) = 0$. The integral term in this equation represents the arrival of cells from M -phase.

2.2. Unperturbed cell lines and Steady DNA Distributions (SDD's)

Tumour cell lines which are unperturbed by radiation or anticancer drugs typically have an unchanging DNA profile over time. In this case we use the terminology steady DNA distribution or SDD. In addition, unperturbed cell lines generally have low rates of cell death. The model equations for an unperturbed cell line are gained by taking the generalised model equations from section 2.1 and setting the transition rate to A -phase, of cells that have been in M -phase for τ_M hours, μ_M , to zero:

$$\frac{\partial G_1}{\partial t}(x, t) = 4bM(2x, t) - k_1 G_1(x, t), \quad (29)$$

$$\frac{\partial S}{\partial t}(x, t) = D \frac{\partial^2 S}{\partial x^2} - g \frac{\partial S}{\partial x}(x, t) + k_1 G_1(x, t) - \bar{S}(x, t; T_S), \quad (30)$$

$$\frac{\partial G_2}{\partial t}(x, t) = \bar{S}(x, t; T_S) - k_2 G_2(x, t), \quad (31)$$

$$\frac{\partial M}{\partial t}(x, t) = k_2 G_2(x, t) - bM(x, t), \quad (32)$$

where side conditions are those given in section 2.1. Equation (32) represents M -phase cells. The cells enter M -phase from G_2 -phase with probability k_2 per unit time and exit M -phase when they divide with division rate b per unit time.

In [2] we used the method of finite differences to solve equations (29)–(32) and hence find the SDD's in each phase. However the method of finite differences becomes impractical for certain parameter values. In this section we look for separable solutions which allow us to find SDD's directly as opposed to asymptotically. We now prove, by using the method of separation of variables, that our model for unperturbed cell lines has separable solutions. We set

$$G_1(x, t) = y_1(x)N(t), \quad (33)$$

$$S(x, t) = y_S(x)N(t), \quad (34)$$

$$G_2(x, t) = y_2(x)N(t), \quad (35)$$

$$M(x, t) = y_M(x)N(t), \quad (36)$$

and emphasise that $y_1(x)$, $y_S(x)$, $y_2(x)$ and $y_M(x)$ represent the SDD solution mode in G_1 , S , G_2 and M -phase respectively. From equations (23) and (24) (with $\tau_S = T_S$ and $g = 1/T_S$),

$$\bar{S}(x, t; T_S) = \begin{cases} k_1 H(t - T_S) G_1(x - 1, t - T_S), & D = 0, \\ k_1 H(t - T_S) \int_0^L G_1(z, t - T_S) \gamma(x, z; T_S) dz, & D \neq 0, \end{cases} \quad (37)$$

where the Heaviside unit step function, $H(t - T_S)$, is equal to 1 for $t \geq T_S$ and zero otherwise. Thus, when $t \geq T_S$, we may write

$$\bar{S}(x, t; T_S) = k_1 N(t - T_S) Y_1(x, T_S), \quad (38)$$

where

$$Y_1(x, T_S) = \begin{cases} y_1(x-1), & D = 0, \\ \int_0^L y_1(z)\gamma(x, z; T_S)dz, & D \neq 0. \end{cases} \quad (39)$$

Substituting equations (33)–(36) and (38) into equations (29)–(32) and on letting λ be the separation constant we have

$$\frac{N'(t)}{N(t)} = \lambda = 4b \frac{y_M(2x)}{y_1(x)} - k_1, \quad (40)$$

$$\frac{N'(t)}{N(t)} = \lambda = D \frac{y_S''(x)}{y_S(x)} - g \frac{y_S'(x)}{y_S(x)} + k_1 \frac{y_1(x)}{y_S(x)} - k_1 \frac{N(t-T_S)}{N(t)} \frac{Y_1(x, T_S)}{y_S(x)}, \quad (41)$$

$$\frac{N'(t)}{N(t)} = \lambda = k_1 \frac{N(t-T_S)}{N(t)} \frac{Y_1(x, T_S)}{y_2} - k_2, \quad (42)$$

$$\frac{N'(t)}{N(t)} = \lambda = k_2 \frac{y_2(x)}{y_M(x)} - b, \quad (43)$$

where the prime denotes differentiation with respect to the function argument. The separation constant, λ , will be a time constant governing the growth of the cell cohort. In equations (40) and (43), the variables separate easily giving $N(t) = N_0 e^{\lambda t}$. This in turn gives

$$\frac{N(t-T_S)}{N(t)} = e^{-\lambda T_S}, \quad (44)$$

thus ensuring the complete separation of variables in the remaining equations (41) and (42).

Substituting equation (44) into equations (40)–(43) and rearranging leads to the following delay equation (45), when $D = 0$, and Fredholm integral equation (46), for the case where $D \neq 0$:

$$y_1(x-1) = \Lambda y_1\left(\frac{x}{2}\right), \quad x > 0, \quad D = 0, \quad (45)$$

$$\int_0^L \gamma(2x, z; T_S) y_1(z) dz = \Lambda y_1(x), \quad 0 < x < L, \quad D \neq 0, \quad (46)$$

where

$$\Lambda = F(\lambda) = \frac{(\lambda + k_1)(\lambda + k_2)(\lambda + b)e^{\lambda T_S}}{4bk_1k_2} \quad (47)$$

is determined as an eigenvalue of equations (45) and (46), and $y_1(x)$ is the corresponding eigenfunction. Note that all parameters are non-negative. Taking the limit as $D \rightarrow 0$ of equation (46) gives equation (45), that is, γ is a δ -sequence as $D \rightarrow 0^+$.

We will solve equations (45) and (46) to obtain a discrete set of eigenvalues $\Lambda = \{\Lambda_0, \Lambda_1, \dots\}$ and a set of corresponding eigenfunctions. These eigenfunctions are the candidates for $y_1(x)$, the steady DNA distribution of the G_1 -phase

cells. We will see that, for both the cases $D = 0$ and $D \neq 0$, the largest eigenvalue, denoted Λ_0 , is simple and corresponds to a positive eigenfunction, $y_1(x)$. In the case $D = 0$ there is only one simple eigenvalue and therefore the corresponding eigenfunction is unique. In the case $D \neq 0$, there are many eigenvalues and so there may be other positive eigenfunctions. We cannot guarantee uniqueness in this latter case. However, numerical investigation suggests that the eigenfunction appears to be unique.

Once the positive eigenfunction, $y_1(x)$, and corresponding eigenvalue, Λ_0 , has been found we then find the critical values of λ , denoted $\tilde{\lambda}$, which satisfy the equation $\Lambda_0 = F(\lambda)$ (equation (47)). The function $F(\lambda)$ is a cubic polynomial with zeros at $-b$, $-k_2$ and $-k_1$, multiplied by an exponential (see equation (47) and Fig. 2). A horizontal line through Λ_0 intersects $F(\lambda)$ in either 1, 2 or 3 places, thus $\tilde{\lambda}$ can take on 1, 2 or 3 possible values. If $F(0) < \Lambda_0$, then there is only one intersection of the curve $F(\lambda)$ and a horizontal line through Λ_0 at the value $\tilde{\lambda}$. The value of $\tilde{\lambda}$ will be positive and this will correspond to population growth. Thus, in mathematical and intuitive terms, a necessary and sufficient condition for population growth is:

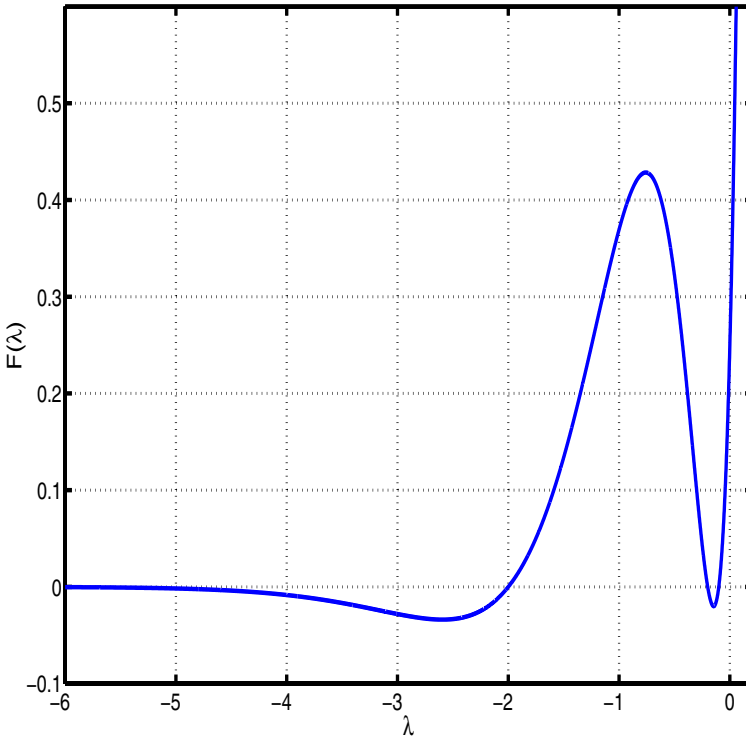


Fig. 2. Plot of $F(\lambda)$, equation (47), as a function of λ as given by equation (47) where $k_1 = 0.1$, $k_2 = 0.2$, $b = 2$ and $g = 0.4$.

$$\begin{aligned}
 F(0) &= \frac{1}{2} \left(\frac{k_1}{2b} \right) \times \left(\frac{1}{k_1} \right) \times \left(\frac{k_2}{1} \right) \times \left(\frac{b}{k_2} \right) \\
 &= \frac{1}{2} \left(\frac{\text{rate out } G_1}{\text{rate in } G_1} \right) \times \left(\frac{\text{rate out } S}{\text{rate in } S} \right) \times \left(\frac{\text{rate out } G_2}{\text{rate in } G_2} \right) \times \left(\frac{\text{rate out } M}{\text{rate in } M} \right) \\
 &< \Lambda_0.
 \end{aligned} \tag{48}$$

We will see that in the case $D = 0$, $\Lambda_0 = 0.5$ and in the $D \neq 0$ case, numerical investigation suggests $\Lambda_0 \sim 0.5$, ensuring population growth for the unperturbed system (since $F(0) = 0.25$). Substituting $\Lambda_0 = 0.5$ into inequality (48), our intuitive condition for population growth is that the product of the outgoing rates must be smaller than the product of the incoming rates. i.e.

$$\begin{aligned}
 &(\text{rate out } G_1) \times (\text{rate out } S) \times (\text{rate out } G_2) \times (\text{rate out } M) \\
 &< (\text{rate in } G_1) \times (\text{rate in } S) \times (\text{rate in } G_2) \times (\text{rate in } M).
 \end{aligned} \tag{49}$$

To gain the steady DNA distribution of the other phases we solve the following equations (obtained via equations (40)–(43)):

$$4by_M(2x) - (\tilde{\lambda} + k_1)y_1(x) = 0, \quad 0 < x < L, \tag{50}$$

$$k_2y_2(x) - (\tilde{\lambda} + b)y_M(x) = 0, \quad 0 < x < L, \tag{51}$$

$$\begin{aligned}
 Dy_S''(x) - gy_S'(x) - \tilde{\lambda}y_S(x) + \\
 k_1y_1(x) - (\tilde{\lambda} + k_2)y_2(x) = 0, \quad 0 < x < L,
 \end{aligned} \tag{52}$$

$$Dy_S'(0) - gy_S(0) = 0, \quad 0 < \int_0^L y_S(x)dx < \infty, \quad 0 < x < L, \tag{53}$$

$$Dy_S'(L) - gy_S(L) = 0, \quad 0 < \int_0^L y_S(x)dx < \infty, \quad 0 < x < L. \tag{54}$$

It should be noted that equation (52) with side conditions (53) and (54), is a linear two point boundary value problem. To ensure the positivity of y_M and y_2 in equations (50) and (51), we must specify that $\tilde{\lambda} > -k_1$ and $\tilde{\lambda} > -b$ respectively and this in turn specifies that $\tilde{\lambda}$ is the only positive root of the equation $F(\lambda) = \Lambda_0$. Thus y_S , y_2 and y_M are able to be determined in terms of the previously determined $y_1(x)$. Since $\tilde{\lambda}$ is positive, this corresponds to population exponential growth.

For the total cell cohort we incorporate all phases and the SDD is given by

$$y_T(x) = y_1(x) + y_S(x) + y_2(x) + y_M(x), \tag{55}$$

where

$$\int_0^L y_T(x)dx = 1, \tag{56}$$

and

$$n(x, t) = N_0y_T(x)e^{\tilde{\lambda}t} = N_0(y_1(x) + y_S(x) + y_2(x) + y_M(x))e^{\tilde{\lambda}t} \tag{57}$$

is the asymptotic (assuming $n(x, t)$ is an attracting solution) form of the total cell cohort. Thus

$$\tilde{\lambda} \gtrsim 0, \quad (58)$$

determines the growth/decay of the cell cohort. Obviously this threshold will depend on the model parameters (k_1, k_2, b, g, D etc).

2.2.1. The no dispersion case ($D = 0$): The eigenvalue problem from equation (45),

$$y(x-1) = \Lambda y\left(\frac{x}{2}\right), \quad (59)$$

is the calculation of Λ for which there are non-negative solutions with support $\{x : x \geq 0\}$. Simple integration of equation (59), shows it has solutions for which $\int_0^L y_1(x) \neq 0$, iff $\Lambda = \Lambda_0 = 0.5$. Thus we have a unique eigenvalue. We then solve the equation in the space of Schwarz's distributions (see [15]). Writing $\hat{y}(u)$ as the Fourier transform of $y(x)$, we get from equation (59),

$$e^{iu} \hat{y}_1(u) = 2\Lambda_0 \hat{y}_1(2u) = \hat{y}_1(2u). \quad (60)$$

Accordingly,

$$\hat{y}_1(u) = e^{(\frac{1}{2} + \frac{1}{4} + \frac{1}{8} + \dots)iu} \hat{y}_1(0) = e^{iu} \hat{y}_1(0), \quad (61)$$

which gives

$$y_1(x) = c_1 \delta(x-1), \quad c_1 \in \mathbf{R}^+. \quad (62)$$

This shows that the long term SDD in G_1 -phase is a point distribution centred at $x = 1$. Similarly from equations (50) - (52), $y_2(x)$ and $y_M(x)$ are point distributions centred at $x = 2$, and $y_S(x)$ is a sum of two Heaviside functions:

$$y_M(x) = c_1 \frac{(\tilde{\lambda} + k_1)}{2b} \delta(x-2), \quad (63)$$

$$y_2(x) = c_1 \frac{(\tilde{\lambda} + k_1)(\tilde{\lambda} + b)}{2k_2b} \delta(x-2), \quad (64)$$

$$\begin{aligned} y_S(x) &= c_1 \left[\frac{k_1}{g} e^{\frac{-\tilde{\lambda}}{g}(x-1)} \mathbf{H}(x-1) \right. \\ &\quad \left. - \frac{(\tilde{\lambda} + k_1)(\tilde{\lambda} + k_2)(\tilde{\lambda} + b)}{2bk_2g} e^{\frac{-\tilde{\lambda}}{g}(x-2)} \mathbf{H}(x-2) \right] \\ &= c_1 \left[\frac{k_1}{g} e^{\frac{-\tilde{\lambda}}{g}(x-1)} \mathbf{H}(x-1) - \frac{2k_1}{g} F(\tilde{\lambda}) e^{\frac{-\tilde{\lambda}}{g}(x-2)} \mathbf{H}(x-2) \right]. \quad (65) \end{aligned}$$

By substituting $F(\tilde{\lambda}) = \Lambda = 0.5$ into equation (65) and $g = 1/T_S$ we may rewrite the solution for $y_S(x)$ more succinctly as:

$$y_S(x) = c_1 k_1 T_S e^{-\tilde{\lambda} T_S (x-1)} (\mathbf{H}(x-1) - \mathbf{H}(x-2)). \quad (66)$$

The constant c_1 can be found by using the property (equation (56)) $\int_0^L y_T(x) dx = 1$, giving

$$c_1 = \left(1 + \frac{\tilde{\lambda} + k_1}{2b} \left(1 + \frac{\tilde{\lambda} + b}{k_2} \right) + \frac{k_1}{\tilde{\lambda}} \left(1 - e^{-\tilde{\lambda}Ts} \right) \right)^{-1}. \quad (67)$$

Since $\tilde{\lambda}$ is unique, the constant c_1 in equation (67) will specify unique distributions in each phase and hence a unique SDD for the case $D = 0$.

2.2.2. The dispersion case $D \neq 0$: In section 2.2.1 we saw that when $D = 0$, the SDD solution in the G_1 -phase was a point distribution. In this section we will see that when D becomes non-zero it acts as a smoothing parameter so that the point distributions are smoothed out into classical distributions.

We would like to ensure the existence of a positive eigenfunction and here we make use of the following theorem due to Jentzsch (see [6] page 256) for the homogeneous Fredholm integral equation:

$$\int_0^L k(x, s)u(s)ds = -\Lambda u(x). \quad (68)$$

Theorem 1. Jentzsch's Theorem. *Let $k(x, s)$ be continuous and positive on $0 \leq x, s \leq L$. Let Λ_0 be the largest eigenvalue of equation (68), then all other eigenvalues are smaller than Λ_0 in absolute value and Λ_0 is simple (i.e., there is only one independent eigenfunction associated with Λ_0). The eigenfunction associated with Λ_0 is positive.*

It is not surprising that the first eigenfunction is positive (see for example [11]), here Jentzsch's theorem ensures the existence (but not uniqueness) of a suitable candidate for y_1 the SDD in G_1 -phase and the corresponding eigenvalue of our Fredholm integral equation (46), Λ_0 .

2.2.3. Numerical Methods for finding the SDD in the $D \neq 0$ case: We first describe the numerical algorithm used to solve the eigenvalue problem described by the Fredholm integral equation (68). The algorithm chosen is simple and of low order but it suffices to solve the eigenvalue problem rapidly and to the desired accuracy.

Define the natural numbers $i, j, M, N \in \mathbb{N}$, and then a mesh $\{x_i\}_{i=0}^N$, with uniform mesh interval $h = L/N$, and $x_0 = 0$, $x_i = x_{i-1} + h$, $1 \leq i \leq N$, is established on the x -axis. Now we initially describe the collocation algorithm to solve the eigenvalue problem for the homogeneous integral equation

$$\Lambda u(x) + \int_0^L k(x, s)u(s) ds = 0, \quad x \in [0, L]. \quad (69)$$

The function $u(x)$ is approximated by a B-spline of degree n , from the linear space of B-splines of degree n , denoted by \mathcal{S}_n , such that

$$u(x) = \sum_{i=0}^M \alpha_i b_i(x), \quad (70)$$

where $M + 1$ is the cardinality of the B-spline basis, $\{b_i(x)\}_{i=0}^M \in \mathcal{S}_n[0, L]$ and $\{\alpha_i\}_{i=0}^M \in \mathbb{R}$. Collocation of the equation (69) then provides the finite dimensional equation

$$\Lambda \alpha_j + \sum_{i=0}^M \alpha_i \int_0^L k(x_j, s) b_i(s) ds = 0, \quad j \in [0, N]. \quad (71)$$

For a concrete implementation of the algorithm here, the integral is approximated by the composite trapezoidal rule on the nodes x_ℓ , and n is chosen to be one; so that the B-spline basis functions are the piecewise linear, or *hat*, functions. Now $M = N$, and denote $k(x_j, s_i)$ by $k_{j,i}$, then (71) can be written as

$$\Lambda \alpha_j + h \sum_{i=0}^M \sum_{\ell=1}^N \alpha_i k_{j,\ell} \delta_{i,\ell} = 0, \quad j \in [0, N], \quad (72)$$

$$\Lambda \alpha_j + h \sum_{i=0}^N \alpha_i k_{j,i} = 0, \quad (73)$$

where use has been made of the fact that $b_i(s_\ell) = \delta_{i\ell}$, with $\delta_{i\ell}$ denoting the Kronecker delta, and the double prime on the summation sign is to signify that the first and last value in the summation is to be halved. From this discretization it is necessary to find the eigenvalues Λ that lead to a non-trivial solution. The expansion algorithm, as implemented, for the eigenfunctions with B-splines of degree one is equivalent to the Nyström method for Fredholm eigenvalue problems. It follows that for the repeated trapezoidal rule, the eigenvalues converge as $\mathcal{O}(h^2)$ ([3]).

The kernel matrix is of small bandwidth, to a given accuracy, because the kernel function is of approximately finite support; this follows from observing from equation (103) that the exponential term has nearly compact support, *i.e.* the exponential function is very nearly zero outside $\pm 3\sqrt{4D\tau}$ of the centre: $x - g\tau$. This means that sparse matrix techniques can be used to find a few of the eigenvalues and associated eigenvectors. In particular the sparse eigenfunction package *eigs* that is available in **Matlab** is utilized for our numerical implementation. This function utilizes the implicitly re-started Arnoldi iteration algorithms from the Fortran library ARPACK. When running this algorithm on an AMD2000+ CPU with $N = 600$ the largest eigenvalue and eigenvector are found in around 2 seconds.

This method of finding the SDD solution is superior to solving the time dependent model (equations (29)–(32)) using finite difference methods, as was done in [2], because the time it takes for the model to converge to a SDD becomes large as parameter values become small and the numerical solution becomes impractical. We should also note that when equation (46) was solved using the numerical methods described in this section, for different parameter values, the eigenvalue, Λ_0 , always had approximately the same constant value, $\Lambda_0 \sim 0.5$. We can compare this to the $D = 0$ case (section 2.2.1) where we have $\Lambda_0 = 0.5$ and to the intuitive meaning of $F(0)$ described in equation (49).

From here we use the **Matlab** function *fzero* (starting at $\lambda = 0.01$) to solve $F(\lambda) = \Lambda_0$ to find $\tilde{\lambda}$, the only positive root of the equation $F(\lambda) - \Lambda_0 = 0$. We

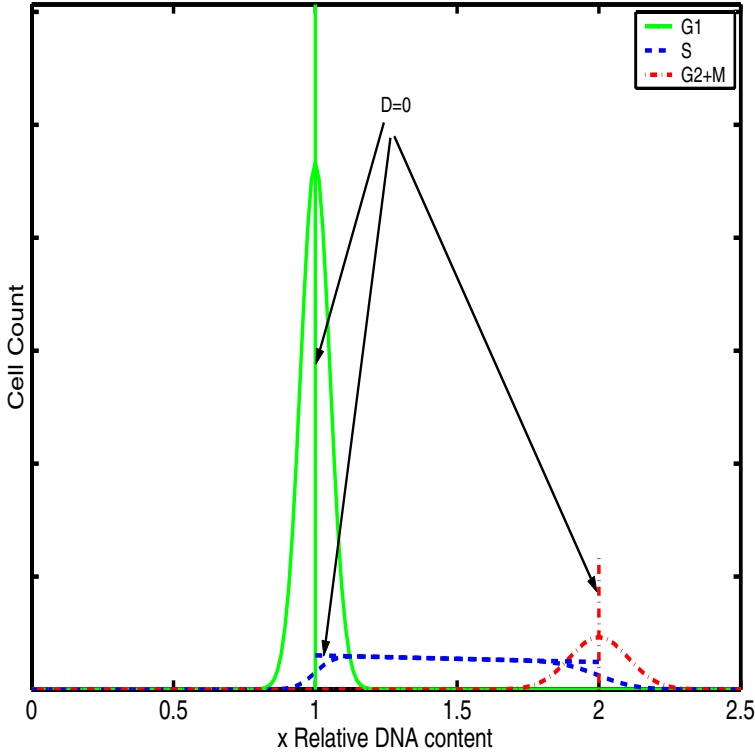


Fig. 3. The SDD solutions of the model for unperturbed cell lines (equations (29)–(32)) have been plotted for the cases $D = 0$ and $D \neq 0$, illustrating the smoothing effect that D has on the SDD. The heights of the point distributions in G_1 , G_2 and M -phase are the constants of multiplication in equations (62)–(64). Arbitrary parameter values are $k_1 = 0.05$, $k_2 = 0.2$, $b = 2$, $D = 4 \times 10^{-4}$, $g = 0.1$, $x_{min} = 0$, $x_{max} = 4$, $\Delta x = 0.1$ ($D = 0$), $\Delta x = 0.0133$ ($D \neq 0$), $F(\lambda) = 0.5 \Rightarrow \lambda = 0.0218$.

may proceed to find the SDD solutions in the remaining S , G_2 and M -phases by solving equations (50)–(52) and hence the total separable SDD solution. To find $y_S(x)$, the SDD solution in S -phase, an approximation of the auxiliary boundary value problem (equations (52)–(54)) was solved using the **Matlab** solver *ode23t*.

In Fig. 3, the SDD solutions of the model for unperturbed cell lines (with arbitrary parameter values) have been plotted for the cases $D = 0$ and $D \neq 0$, illustrating the smoothing effect that D has on the SDD.

2.2.4. Uniqueness and attractiveness of SDD solutions: For the case $D = 0$ we have found a unique positive separable solution for the total DNA distribution, $n(x, t)$. For the case $D \neq 0$ we have found one positive separable solution but there may be others. In both cases $D = 0$ and $D \neq 0$ we state the following conjectures:

1. there may be other types of non-separable solutions,
2. we have assumed that our separable solutions are attracting.

Conjectures 1. and 2. have not been proven and will be the subject of further investigations.

2.3. Modelling a cell line perturbed by the anticancer drug paclitaxel

Paclitaxel, given at a high enough concentration, causes the complete arrest of cells in M -phase and the subsequent induction of apoptosis. Flow cytometry suggests that cells build up in G_2/M -phase and then after a time these cells may undergo apoptosis. To model the addition of paclitaxel we start with a steady DNA profile, set the division rate parameter b to zero and set the transition rate to A -phase from M -phase, μ_M to a non-zero value when $t \geq T_M$. We assume that cells stay in M -phase for T_M hours before the onset of apoptosis. Using the notation from section 2.1, the model equations for a cell line perturbed by paclitaxel are summarised:

$$\frac{\partial G_1}{\partial t}(x, t) = -k_1 G_1(x, t), \quad (74)$$

$$\begin{aligned} \frac{\partial S}{\partial t}(x, t) = D \frac{\partial^2 S}{\partial x^2} - g \frac{\partial S}{\partial x}(x, t) \\ + k_1 G_1(x, t) - \bar{S}(x, t; T_S), \end{aligned} \quad (75)$$

$$\frac{\partial G_2}{\partial t}(x, t) = \bar{S}(x, t; T_S) - k_2 G_2(x, t), \quad (76)$$

$$\frac{\partial \bar{M}}{\partial t}(x, t; \tau_M) + \frac{\partial \bar{M}}{\partial \tau_M}(x, t; \tau_M) = -\mu_M \bar{M}(x, t; \tau_M), \quad (77)$$

$$M(x, t) = \int_0^\infty \bar{M}(x, t; \tau_M) d\tau_M, \quad (78)$$

$$\begin{aligned} \frac{\partial A}{\partial t}(x, t) = \frac{\partial (g_A A)}{\partial x}(x, t) \\ + \int_{T_M}^t \mu_M \bar{M}(x, t; \tau_M) d\tau_M, \end{aligned} \quad (79)$$

where $0 < x < L$ and $t, \tau_M > 0$. Initial and boundary conditions are:

$$G_1(x, 0) = G_{10}(x), \quad 0 < x < L, \quad (80)$$

$$S(x, 0) = S_0(x), \quad 0 < x < L, \quad (81)$$

$$D \frac{\partial S}{\partial x}(0, t) - gS(0, t) = 0, \quad t > 0, \quad (82)$$

$$D \frac{\partial S}{\partial x}(L, t) - gS(L, t) = 0, \quad t > 0, \quad (83)$$

$$G_2(x, 0) = G_{20}(x), \quad 0 < x < L, \quad (84)$$

$$\bar{M}(x, t; \tau_M = 0) = k_2 G_2(x, t), \quad 0 < x < L, \quad t > 0, \quad (85)$$

$$\bar{M}(x, t = 0; \tau_M) = \bar{M}_{0\tau_M}(x, \tau_M), \quad \tau_M > 0, \quad 0 < x < L, \quad (86)$$

$$\begin{aligned}
 M(x, 0) = M_0(x) &= \int_0^\infty \bar{M}(x, 0; \tau_M) d\tau_M \\
 &= \int_0^\infty \bar{M}_{0\tau_M}(x, \tau_M) d\tau_M, & 0 < x < L, & \quad (87)
 \end{aligned}$$

$$A(x, 0) \equiv 0, \quad 0 < x < L, \quad (88)$$

$$A(0, t) = 0, \quad t > 0, \quad (89)$$

where $G_{10}(x)$, $S_0(x)$, $G_{20}(x)$ and $M_0(x)$, the initial distributions in G_1 , S , G_2 and M -phase respectively at time $t = 0$, represent the starting point for an experiment and are the SDD solutions obtained from the model of an unperturbed cell line.

The model for a cell line perturbed by paclitaxel does not display SDD behaviour in the sense that we cannot express the total DNA distribution as $n_T(x, t) = N_0 e^{\lambda t} y_T(x)$ as we did with the model for an unperturbed cell line. This can be seen firstly by considering equation (74) which indicates that $G_1(x, t) \sim e^{-k_1 t}$. However, substituting this (by way of $\bar{S}(x, t; T_S)$) into equation (76), we see that $G_2(x, t) \sim e^{-(k_2+k_1)t}$. If we assume that k_2 is strictly positive, then there are different rates of population decay in the G_1 and G_2 phases and similarly for the other phases. Asymptotically, the DNA distribution in each phase, and hence the total distribution tends to zero. This is because, without cell division, cells progress through G_1 , S , G_2 and M -phase where they accumulate for at least T_M hours before entering A -phase. Once in A -phase the DNA continues to degrade until it can no longer be detected by the flow cytometer. Here we have accounted for this by the boundary condition (89) $A(0, t) = 0$. This corresponds to cells exiting the system.

The parameters T_M , μ_M and $g_A(x)$ provide the possibility of measuring the time spent in M -phase before the onset of apoptosis, the rate that cells enter A -phase and the degradation rate respectively. The proportion of M -phase cells entering A -phase at time t is given by the expression:

$$\frac{\mu_M \int_{T_M}^t \bar{M}(x, t; \tau_M) d\tau_M}{\left(\int_0^{T_M} k_2 G_2(x, t - \tau_M) d\tau_M + \int_{T_M}^t \bar{M}(x, t; \tau_M) d\tau_M \right)}, \quad (90)$$

which tends to μ_M as $t \rightarrow \infty$, since $G_2(x, t) \rightarrow 0$ as $t \rightarrow \infty$. Thus we can call μ_M the eventual rate of entry of M -phase cells into A -phase.

3. The optimisation

For the model of a cell line perturbed by paclitaxel, our aim is to find the least square error between the experimental DNA distributions and total DNA distributions predicted by the model. Consequently, we define the objective function, $\psi(\beta)$, as

$$\psi(\beta) = \sum_{j=1}^{\mathcal{J}} \sum_{i=1}^{\mathcal{I}} \left(n_T(x_i, t_j) - Data(x_i, t_j) \right)^2, \quad (91)$$

where β is a vector of model parameters,

$$n_T(x_i, t_j) = G_1(x_i, t_j) + S(x_i, t_j) + G_2(x_i, t_j) + M(x_i, t_j) + A(x_i, t_j)$$

is the total number density of cells with DNA content x_i at time t_j and $Data(x_i, t_j)$ is the corresponding data point. Our aim is to minimise $\psi(\beta)$, with respect to β , i.e. by variation of a fixed set of model parameters over their expected range of values.

In this paper we consider one particular melanoma cell line, denoted NZM13 or New Zealand melanoma-13 ([13]). We choose to minimise the objective function, equation (91), over the parameter set $\beta = [k_1, k_2, T_M(\text{scaled}), \mu_M, g_A]$, where k_1 and k_2 are the transition rates from G_1 -phase to S -phase and G_2 -phase to M -phase respectively. T_M is the time in M -phase before the onset of A -phase, μ_M is the eventual transition rate of cells from M -phase to A -phase and g_A is the degradation rate during A -phase. These parameters are chosen because they are the most difficult to estimate experimentally. The parameter T_M is scaled by a factor of 1×10^{-3} during the optimisation so that it has the same order of magnitude as the other parameters. When presenting results we will only refer to the parameter T_M without scaling. Remaining model parameters are fixed at the values: $D = 4 \times 10^{-4}$, $g = 0.1$ and $b = 2$, see Table 1. The values of g and b are chosen because the average time that a cell spends in S -phase and M -phase is $T_S = 1/g = 10$ hours and $1/b = 30$ minutes respectively. The value of D can be estimated by comparing model and data profiles prior to the optimisation procedure.

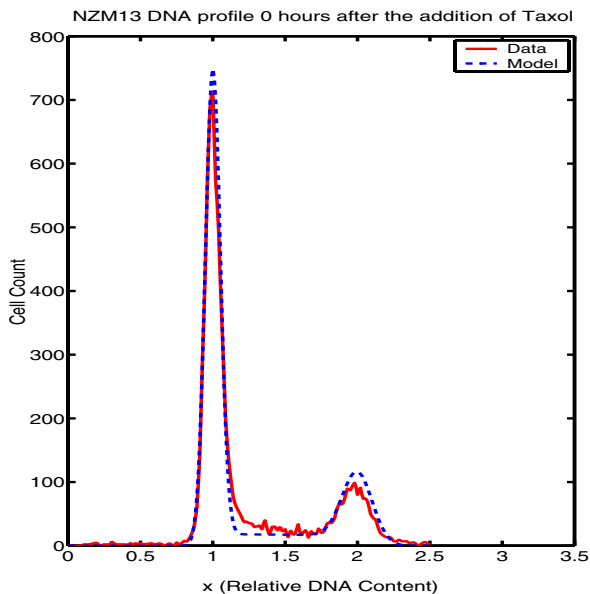
To perform the optimisation, we use the **Matlab** function *fmincon*. We put bounds on certain parameter values as summarised in Table 1. Firstly, the parameters k_1 , k_2 and μ_M represent transition probabilities and therefore lie within the interval $[0,1]$. We require the parameters k_1 and k_2 to be strictly positive and *fmincon* requires a compact interval. We can use rough estimates of the average time in G_1 and G_2 -phase to be $1/k_1$ and $1/k_2$, respectively ([16]). If we enforce the condition that the time in each phase must be less than 250 hours we may choose both parameters, k_1 and k_2 , to lie in the interval $[4 \times 10^{-4}, 1]$. Secondly, T_M is assumed to lie between 0 and 40 hours. Thirdly, the degradation rate, g_A is chosen to lie in the interval $[0, 2/\Delta t]$. The right hand side of this interval is chosen so that it takes more than one time step, Δt , for a cell to degrade its DNA content from $x = 2$ to $x = 0$. Finally, we assume that the total cell cycle time of the unperturbed system (estimated as $T_c = 1/k_1 + 1/g + 1/k_2 + 1/b$) lies between 12 and 250 hours.

During the optimisation, in order to obtain each objective function value, we must first solve the unperturbed system using the methods described in section 2.2.3. We then use the resultant SDD of the unperturbed system as the starting point of the perturbed system as described in section 2.3. For reasons discussed at the beginning of this section, we use the method of finite differences to solve the perturbed system as described in [2]. The model output of the perturbed system is the total DNA profile, $n_T(x, t)$, which can be compared to the data DNA distributions at the appropriate discrete times, t_j , in the least squares sense, giving the objective function value of equation (91).

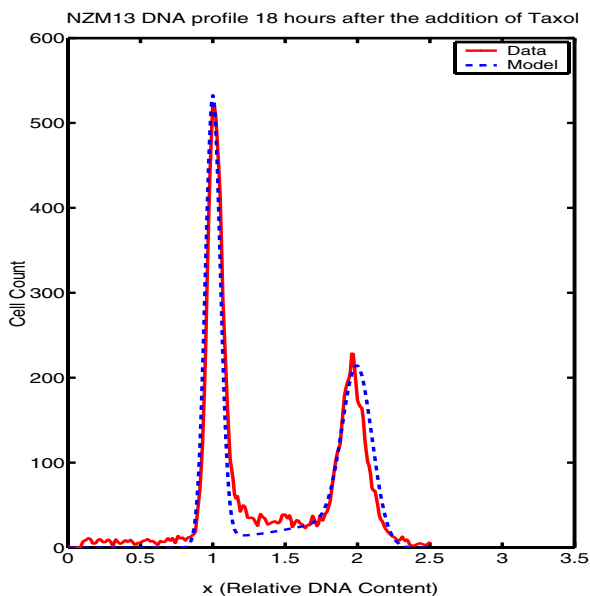
4. Results

4.1. The optimal parameter fit

Figures 4–6 show the optimal fit between model and data for the NZM13 cancer cell line at times 0, 18, 48, 72 and 96 hours after the addition of paclitaxel. As

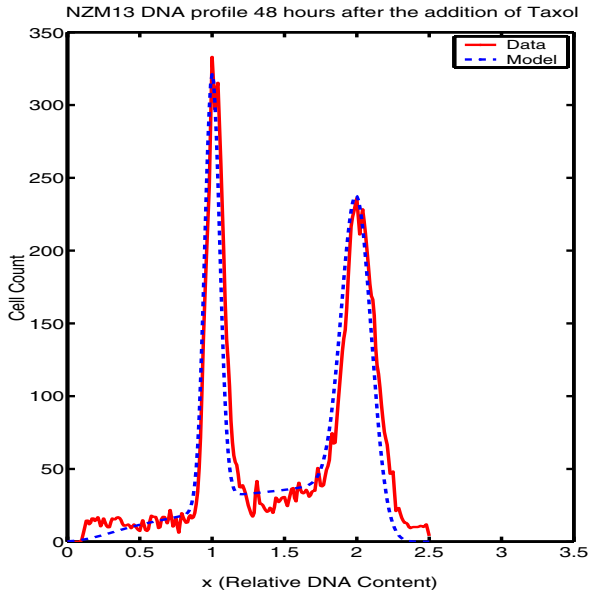


(a)

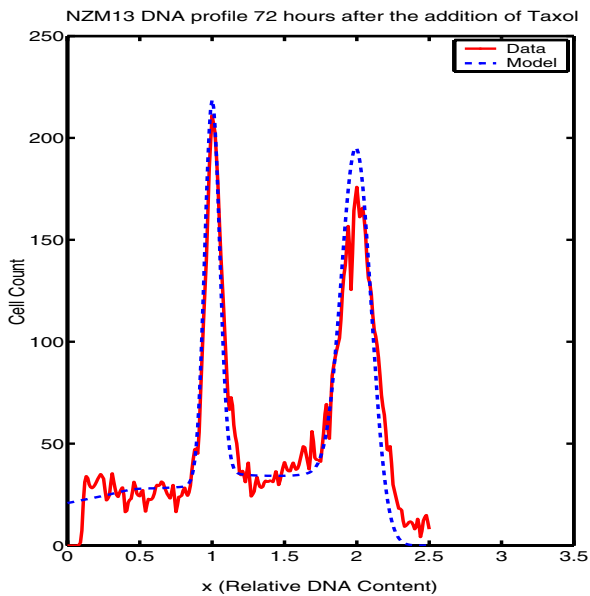


(b)

Fig. 4. Model and experimental DNA distributions for the human cancer cell line NZM13 at times 0 and 18 hours (graphs (a) and (b) respectively) after the addition of paclitaxel. This anticancer drug causes mitotic arrest and the subsequent build up of cells in the G_2/M -phase.



(a)



(b)

Fig. 5. Model and experimental DNA distributions for the human cancer cell line NZM13 at times 48 and 72 hours (graphs (a) and (b) respectively) after the addition of paclitaxel. This anticancer drug causes mitotic arrest and the subsequent build up of cells in the G_2/M -phase.

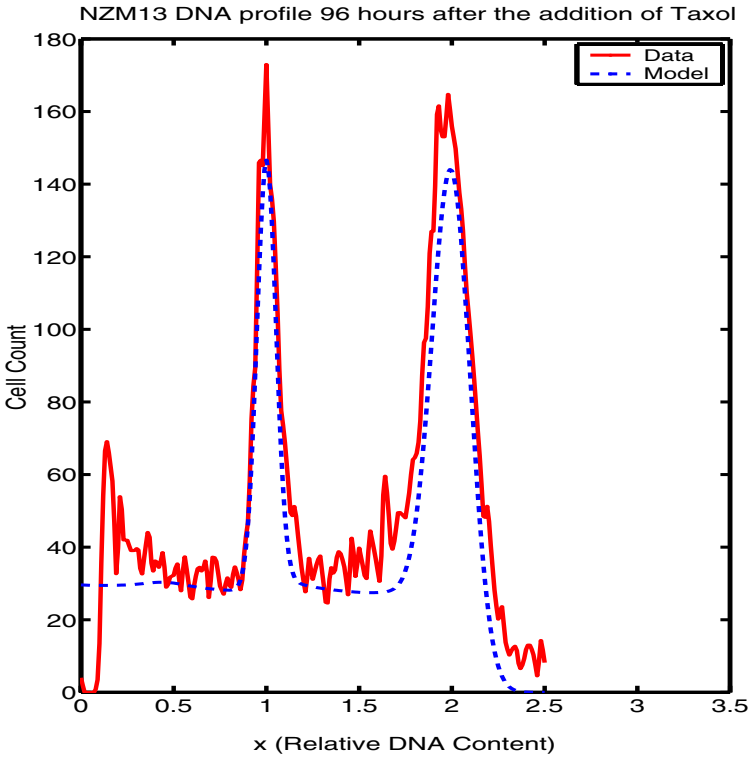


Fig. 6. Model and experimental DNA distributions for the human cancer cell line NZM13 at 96 hours after the addition of paclitaxel. This anticancer drug causes mitotic arrest and the subsequent build up of cells in the G_2/M -phase.

time evolves, cells build up in M -phase. A small peak centred at the DNA content of G_1 -phase cells persists and could suggest the presence of senescent cells (cells that have irreversibly left the cell division cycle). At 18 hours, DNA degradation has already begun, as seen by the accumulation of A -phase cells distributed through both the S -phase region and between the G_1 -phase and the origin. The model enables us to obtain graphs of the percentages and absolute numbers of cells in each phase as a function of time (Fig. 7 and 8 respectively).

The optimal parameter set is $\beta = [k_1 = 0.0191, k_2 = 0.0513, T_M = 0, \mu_M = 0.0354, g_A = 0.0394]$. Thus the model predicts that apoptosis begins immediately ($T_M = 0$) and that the eventual rate of entry of mitotic cells into A -phase tends to $\mu_M = 0.0354$ per hour (Fig. 9). The rate of DNA degradation with time during A -phase is $g_A = 0.0394$. The g_A parameter provides an estimate of the time a cell spends in A -phase. Cells generally enter A -phase with relative DNA content at approximately $x = 2$. Thus the time it takes for a cell to degrade its DNA content to $x = 0$ when the rate of degradation is g_A is $\frac{2}{g_A} \approx 51$ hours. The doubling time, T_d , of the unperturbed system is numerically estimated as $T_d = 71$ hours ($\lambda = \frac{\ln(2)}{T_d} = 0.0090$), agreeing well with an experimentally estimated dou-

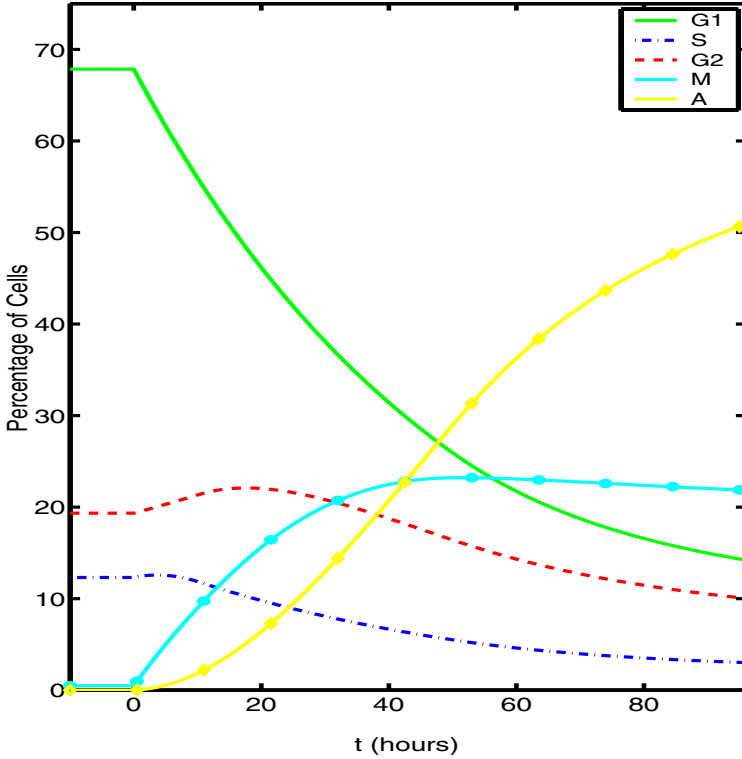


Fig. 7. Percentage of cells in each phase as a function of time as predicted by the model for human cell line NZM13. Division stopped at $t = 0$ hours, prior to this the model had a steady DNA distribution as seen by constant percentages in each phase. Model parameters that were fitted were: k_1 , k_2 , T_M and μ_M and g_A . For parameter descriptions and units see Table 1.

bling time (data not shown) of 3.2 days ($\lambda = 0.0098$). The model assumes that the degradation rate of DNA in A -phase is constant, but the lack of exact fit at lower DNA contents suggests a time dependence of degradation (see section 5).

4.2. Uniqueness of the optimal parameter fit

An exploration of objective function values, expression (91), over the appropriate domain for the parameter values T_M , μ_M and g_A suggest that we have a global optimum. However the objective function seems to have a ‘flat valley’, meaning that certain combinations of the parameters T_M , μ_M and g_A give similar (albeit greater) objective function values and hence a good fit between model and data. Further work may be needed to eliminate biologically unreasonable parameter sets.

5. Biological significance

Paclitaxel, an important anticancer drug used in the treatment of ovarian cancer, causes the arrest of cells in M -phase and the subsequent induction of apoptosis

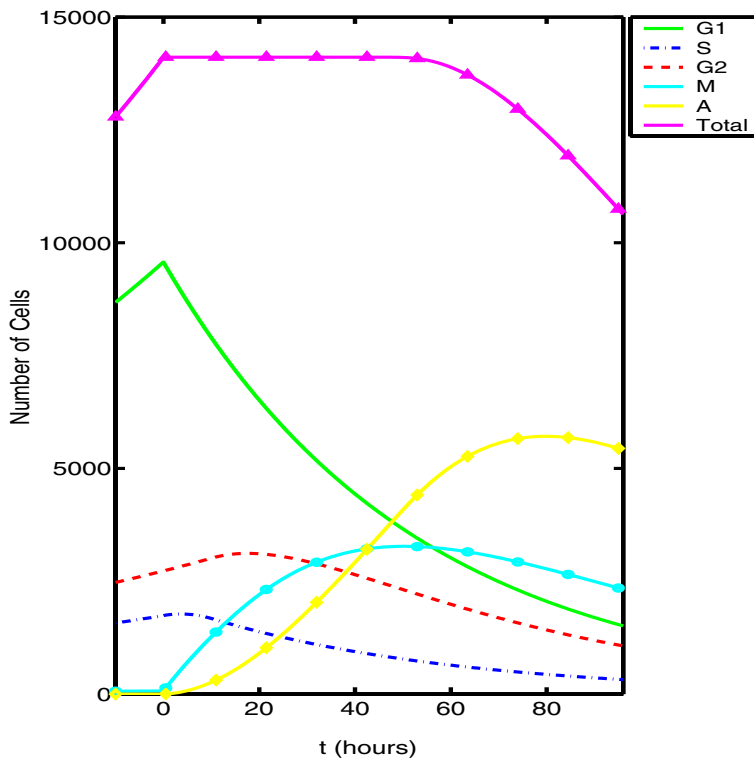


Fig. 8. Number of cells in each phase as a function of time as predicted by the model for human cell line NZM13. Division stopped at $t = 0$ hours, prior to this cells can be seen to be growing exponentially. Model parameters that were fitted were: k_1 , k_2 , T_M and μ_M and g_A . For parameter descriptions and units see Table 1.

([7]). While haemopoietic cells (i.e. of bone-marrow origin) enter apoptosis from interphase (G_1 -phase, S -phase or G_2 -phase), carcinoma and melanoma cells are more likely to enter apoptosis at mitosis by a process called mitotic cell death or mitotic catastrophe ([5]). The present results are consistent with this latter mechanism. A -phase cells, while degrading their DNA, appear to remain close to their original size, as measured by forward scatter measurements in the flow cytometer (data not shown).

The best fit for the model suggests $T_M = 0$, suggesting that once paclitaxel is added, all M -phase cells have a finite chance of entering A -phase. The model also predicts that the rate of entry of cells into A -phase converges to a constant value from an initial higher value (Fig. 9). A possible explanation for these properties is that in the unperturbed population of cycling cells, a proportion of cells (approximately 0.5%) is already in M -phase and may be affected immediately. At subsequent times M -phase cells are generated from the G_2 -phase population. The model predicts that the DNA is degraded progressively over a period of approximately 50 hours. In most descriptions of apoptosis, DNA is degraded by an endonuclease, which causes double-stranded DNA breaks and subsequent DNA fragmentation

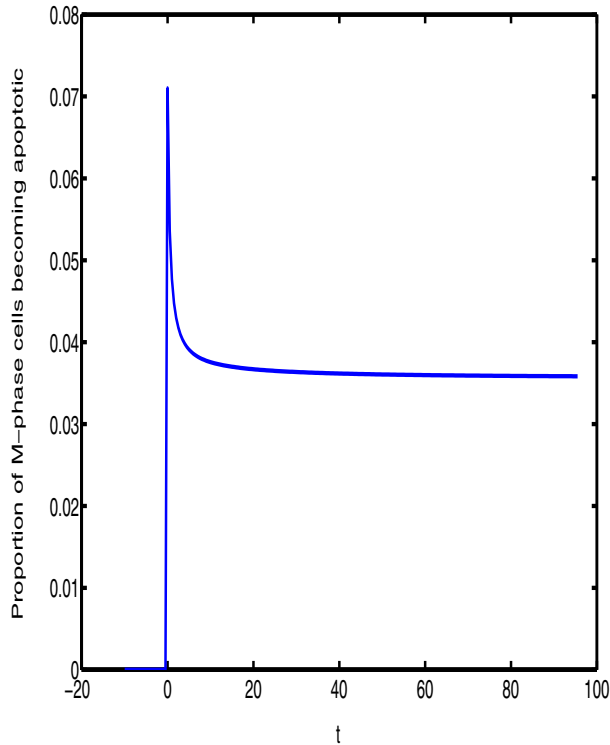


Fig. 9. Model estimation for human cell line NZM13 of the rate of entry of cells into *A*-phase as a function of time. This rate quickly converges to the optimal value of $\mu_M = 0.0394$. For parameter descriptions and units see Table 1.

([14]). However, breakage alone would not cause a decrease in cellular DNA content, and DNA degradation by an exonuclease, which starts with a DNA break and removes DNA bases sequentially, would be more consistent with the observed results. An apoptosis-associated enzyme with both exonuclease and endonuclease functions has been described ([10]). Variations in the balance of exonuclease and endonuclease activities could change the apparent rate of DNA degradation with time, as suggested by the results in Fig. 6.

The mathematical model used here offers a new approach to analysing the effects of paclitaxel, predicting both the changes to cell cycle distribution (Figs. 4-6) and the loss of cells from a population (Fig. 8 and 10). We are currently applying this model to a series of human cancer cell lines in order to determine the extent of variation among cancer lines from different individuals. Human tumours generally have longer cell cycle times than do cell lines ([1]) and one obvious application of the model is to predict the response to paclitaxel and related drugs of human tumours in a clinical setting.

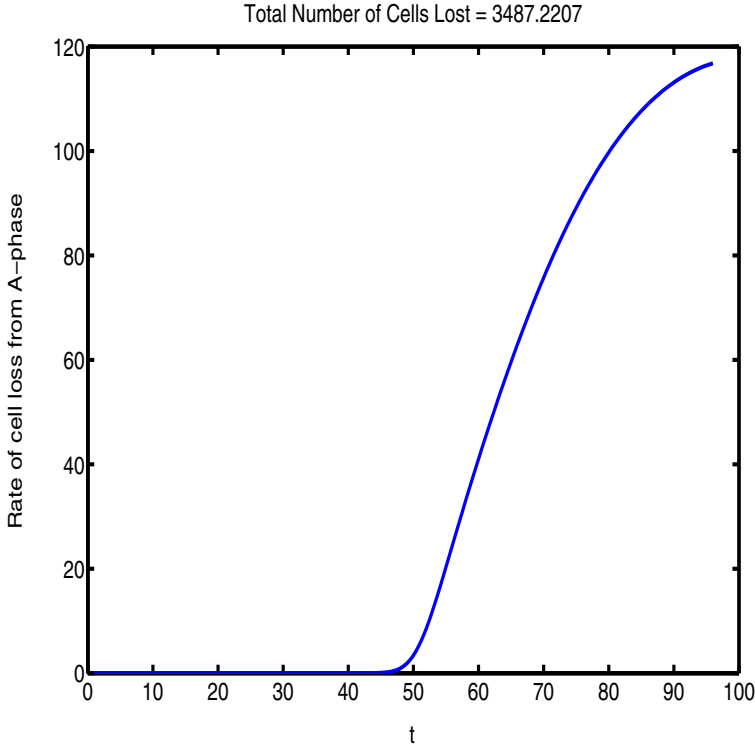


Fig. 10. Model estimation of the rate of eventual cell loss from A-phase as a function of time for human cell line N2M13. Division stopped at $t = 0$ hours. Model parameters that were fitted were: k_1 , k_2 , T_M and μ_M and g_A . For parameter descriptions and units see Table 1.

Acknowledgements. This work was supported by grants from the Auckland Cancer Society (B.C.B, E.S.M), and one of the authors (B.B) acknowledges the receipt of a University of Canterbury post doctoral scholarship.

Appendix: The Green function for the advection diffusion equation

We denote the group of cells, entering S -phase at time t as $\bar{S}(x, t; \tau = 0) = \bar{S}_0(x, t)$. The model assumes that this group of cells simply enter S -phase, double their DNA content (or die) and then exit to the next phase (G_2) without any interaction with cells that enter S -phase at different times. Thus, for a particular time t , the transition of the group of cells into S -phase occurs as an initial condition and the dynamics of any one particular cell group, while in S -phase, are governed by the homogeneous initial-boundary problem:

$$\begin{aligned} \frac{\partial \bar{S}}{\partial t}(x, t; \tau) + \frac{\partial \bar{S}}{\partial \tau}(x, t; \tau) + g \frac{\partial \bar{S}}{\partial x} \\ - D \frac{\partial^2 \bar{S}}{\partial x^2} + \mu_S \bar{S} = 0, \quad 0 < x < L, \quad t, \tau > 0, \end{aligned} \quad (92)$$

with initial and boundary conditions

$$\bar{S}(x, t; \tau = 0) = \bar{S}_0(x, t), \quad 0 < x < L, \quad t \geq 0, \quad (93)$$

$$D \frac{\partial \bar{S}(0, t; \tau)}{\partial x} - g \bar{S}(0, t; \tau) = 0, \quad t, \tau \geq 0, \quad (94)$$

$$D \frac{\partial \bar{S}(L, t; \tau)}{\partial x} - g \bar{S}(L, t; \tau) = 0, \quad t, \tau \geq 0. \quad (95)$$

The parameter τ (in the paper referred to as τ_S) represents the time that a cell has spent in S -phase. For future reference we have included a parameter μ_S representing possible cell loss (death) from S -phase -in the paper we have assumed that $\mu_S = 0$.

In all problems of interest here the diffusion coefficient, D , is very small, and of the order 10^{-4} ; this will mean the second order derivative term can be considered as a singular perturbation in the partial differential equation and the boundary conditions. Therefore, to first order we will assume that the boundary conditions (equations (94) and (95)) can be approximated by the Dirichlet conditions $\bar{S}(0, t; \tau) = 0$ and $\bar{S}(L, t; \tau) = 0$ respectively.

To find an analytic solution to equation (92) we transform the dependent variable

$$\bar{S}(x, t; \tau) = \exp[g(x - g\tau/2)/(2D)]w(x, t; \tau), \quad (96)$$

and then express the problem in characteristic coordinates $w(x, t; \tau) = v(x, r, s)$ where $r = t - \tau$ and $s = \tau$. The equation (92), and the side conditions become

$$\frac{\partial v}{\partial s} - D \frac{\partial^2 v}{\partial x^2} + \mu_S v = 0, \quad 0 < x < L, \quad t, s > 0, \quad (97)$$

$$v(x, r; s = 0) = \bar{S}_0(x, r)e^{-gx/2D}, \quad 0 < x < L, \quad t \geq 0, \quad (98)$$

$$v(0, r; s) = 0, \quad t, s \geq 0, \quad (99)$$

$$v(L, r; s) = 0, \quad t, s \geq 0. \quad (100)$$

The solution for \bar{S} on the quadrant $x, \tau > 0$, with Dirichlet conditions on $x = 0$ and $x = L$ is, by the method of Green functions

$$\bar{S}(x, t; \tau) = \begin{cases} \int_0^L \bar{S}_0(z, t) \gamma(\tau, x, z) dz, & 0 < t < \tau, \quad x > 0, \\ \bar{S}_0(x, t), & \tau = 0, \\ 0, & t < \tau, \end{cases} \quad (101)$$

where

$$\gamma(\tau, x, z) = \frac{e^{-\mu_S \tau} e^{g(x-z-g\tau/2)/(2D)}}{2\sqrt{\pi D \tau}} \times \sum_{n=-\infty}^{\infty} \left(e^{-(x-z+|n|2L)^2/4D\tau} - e^{-(x+z-|n|2L)^2/4D\tau} \right), \quad \tau, x, z > 0, \quad (102)$$

is the Green function for equation (92). Note that we have used the method of images (see [12] or [9] for example) to obtain the Green function in (102).

As the diffusion coefficient is typically very small in this problem, as stated in Table 1, the exponential terms in equation (102) have nearly compact support, *i.e.* the exponential functions are very nearly zero outside $\pm 3\sqrt{4D\tau}$ of the respective centres: $x + |n|2L$ for the first exponential and $-x + |n|2L$ in the second exponential. It is therefore readily seen by examination of the support of x , namely $0 \leq x \leq L$ that the series converges rapidly, and in fact one term suffices to approximate γ as:

$$\gamma(\tau, x, z) \approx \frac{e^{-\mu s \tau}}{2\sqrt{\pi D \tau}} e^{-(x-g\tau-z)^2/4D\tau}, \quad \tau, x, z > 0. \quad (103)$$

Now we justify the replacement of a single flux free boundary condition at $x = 0$ by the Dirichlet boundary condition. To do this we first define the initial condition (98) as $f(x, t; \tau) = \bar{S}_0(x, t)e^{-gx/2D}$, this is prescribed on $0 \leq x < \infty$, and we need continue this as an odd function on $(-\infty, \infty)$ through defining the extension function

$$\begin{aligned} \frac{\partial \tilde{f}}{\partial x}(x, t; \tau) - \frac{g}{2D} \tilde{f}(x, t; \tau) \\ = -D \frac{\partial f}{\partial x}(-x, t; \tau) + \frac{g}{2D} f(-x, t; \tau), \quad -\infty < x < 0. \end{aligned}$$

The solution of this differential equation gives the odd extension of the initial condition as

$$\tilde{f}(x) = f(-x) - \frac{g}{D} e^{gx/2D} \int_0^{-x} e^{gz/2D} f(z) dz, \quad -\infty < x < 0,$$

and integration of the integral by parts yields the following expansion in powers of D/g

$$\begin{aligned} \tilde{f}(x, t; \tau) = & -f(-x, t; \tau) + 2f(0, t; \tau)e^{gx/2D} \\ & + \frac{4D}{g} \left(f'(-x, t; \tau) - f'(0, t; \tau)e^{gx/2D} \right) + \mathcal{O}\left(\left(\frac{D}{g}\right)^2\right), \end{aligned}$$

where $-\infty < x < 0$. With this extension of the initial condition the partial differential equation in (97) is now defined on $(-\infty, \infty)$, and its solution (with $s = \tau$) will be given by

$$v(x, t; \tau) = \begin{cases} \int_0^\infty \bar{S}_0(z, t) e^{-gz/2D} \gamma_v(\tau, x, z) dy + I_{corr}, & t, \tau, x > 0, \\ \bar{S}_0(x, t) e^{-gx/2D}, & \tau = 0, \end{cases}$$

where

$$\gamma_v = \frac{e^{-\mu s \tau}}{2\sqrt{\pi D \tau}} \left(e^{-(x-z)^2/4D\tau} - e^{-(x+z)^2/4D\tau} \right), \quad \tau, x, z > 0,$$

and

$$\begin{aligned} I_{corr} &= 2\bar{S}_0(0, t) \int_0^\infty \gamma_0(\tau, x, -z) dz + \mathcal{O}\left(\frac{D}{g}\right), \\ &= \bar{S}_0(0, t) \left(1 - \operatorname{erf}\left(\frac{x}{2\sqrt{D\tau}}\right)\right) + \mathcal{O}\left(\frac{D}{g}\right) \quad \tau > 0, \end{aligned}$$

with

$$\gamma_0(\tau, x, z) = \frac{e^{-\mu s \tau}}{2\sqrt{\pi D \tau}} e^{-(x-z)^2/4D\tau}, \quad \tau > 0.$$

It is now observed that the asymptotic expansion of the error function for large argument is

$$\operatorname{erf}(x) = 1 - \frac{e^{-x^2}}{\sqrt{\pi}} \frac{1}{x} + \mathcal{O}(x^{-3})$$

so that it follows, except in the small layer region $0 < x < 2\sqrt{D\tau}$, the correction term $I_{corr} \approx 0$. This is as stated above a singular perturbation effect. With D very small and $\tau \approx 10$ (Table 1) it follows the correction term has no significant effect on the numerical calculations so is omitted. It then follows the solution of \bar{S} is obtained via equation (101) with the Green function, γ , being approximated via equation (103). By using similar reasoning we can justify the replacement of the flux free boundary conditions by the Dirichlet boundary condition at $x = L$ and thus the approximation Green function (equation (103)) suffices in all our numerical calculations.

References

1. Baguley, B.C., Marshall, E.S., Finlay, G.J.: Short-term cultures of clinical tumor material: potential contributions to oncology research. *Oncol. Res.* **11**, 115–24 (1999)
2. Basse, B., Baguley, B.C., Marshall, E., Joseph, W.R., van-Brunt, B., Wake, G.C., Wall, D.J.N.: A mathematical model for analysis of the cell cycle in cell lines derived from human tumors. *J. Math. Biol.* **47**, 295–312 (2003)
3. Delves, L.M.: Rayleigh-Ritz-Galerkin Methods chapter 6, pp. 64–79. In Delves and Walsh [4], 1974
4. Delves, L.M., Walsh, J., ed.: Numerical Solution of Integral equations. Clarendon Press, Oxford, 1974
5. Gudkov, A.V., Komarova, E.A.: The role of p53 in determining sensitivity to radiotherapy. *Nature Reviews Cancer* **3**, 117–129 (2003)
6. Hochstadt, H.: Integral Equations. Wiley Interscience, USA, 1973
7. Jordan, M.A., Wendell, K., Gardiner, S., Derry, W.B., Copp, H., Wilson, L.: Mitotic block induced in HeLa cells by low concentrations of paclitaxel (taxol) results in abnormal mitotic exit and apoptotic cell death. *Cancer Res.* **56**, 816–825 (1996)
8. Lengauer, C., Kinzler, K.W., Vogelstein, B.: Genetic instability in colorectal cancers. *Nature* **386**, 623–627 (1997)
9. Mackie, A.G.: Boundary Value Problems. Oliver and Boyd, 1966

10. Meng, X.W., Fraser, M.J., Feller, J.M., Ziegler, J.B.: Caspase-3 activates endonuclease: further evidence for a role of the nuclease in apoptosis. *Apoptosis* **5**, 243–254 (2000)
11. Metz, J.A.J., Diekmann, O.: The dynamics of physiologically structured populations. Number 68. Lecture notes in Bio-mathematics, Springer-Verlag, 1986
12. Morse, P.M., Feshbach, H.: *Methods of Theoretical Physics*. Volume **1**, McGraw-Hill, New York, 1953
13. Parmar, J., Marshall, E.S., Charters, G.A., Holdaway, K.M., Shelling, A.N., Baguley, B.C.: Radiation-induced cell cycle delays and p53 status of early passage melanoma lines. *Oncol. Res.* **12**, 149–155 (2000)
14. Peitsch, M.C., Polzar, B., Stephan, H., Crompton, T., MacDonald, H.R., Mannherz, H.G., Tschopp, J.: Characterization of the endogenous deoxyribonuclease involved in nuclear DNA degradation during apoptosis (programmed cell death). *EMBO J.* **12**, 371–377 (1993)
15. Stakgold, I.: *Green's Functions and Boundary Value Problems*. Wiley-InterScience, New York, 1979
16. Steel, G.G.: *Growth kinetics of tumours* Clarendon. Oxford, 1977
17. Takahashi, M.: Theoretical Basis for cell cycle analysis. II. Further studies on labelled mitosis wave method. *J. Theor. Biol.* **18**, 195–209 (1968)
18. Telford, W.G., King, L.E., Fraker, P.J.: Comparative evaluation of several DNA binding dyes in the detection of apoptosis-associated chromatin degradation by flow cytometry. *Cytometry* **13**, 137–143 (1992)